

## A NUMERICAL ANALYSIS OF BSF LAYERS FOR ULTRA-THIN HIGH EFFICIENCY CdTe THIN FILM SOLAR CELL

M. A. A. NOMAN<sup>a</sup>, S. SIRAJ<sup>a</sup>, M. J. ABDEN<sup>a</sup>, N. AMIN<sup>b,c</sup>, M. A. ISLAM<sup>b,\*</sup>

<sup>a</sup>*Department of Electrical and Electronic Engineering, International Islamic University Chittagong, Chittagong-4314, Bangladesh*

<sup>b</sup>*Institute of Sustainable Energy (ISE), Universiti Tenaga Nasional, Bangi 43000, Selangor, Malaysia*

<sup>c</sup>*Department of Electrical, Electronic and System Engineering, National University of Malaysia, Bangi, 43600, Selangor, Malaysia*

Owing to have an ideal bandgap of 1.45 eV for solar cell fabrication, Cadmium Telluride (CdTe) has gained vast popularity in recent years. However, there is a serious issue under research to make ohmic contact at the back electrode. In this numerical investigation CdS:O/CdTe cell is analyzed with different BSF layers such as As<sub>2</sub>Te<sub>3</sub>, PbTe, SnTe and GeTe which could be resolved the back contacting problem in CdTe solar cells. This comparative investigation is based on the performance of CdTe cell with those mentioned BSF materials in terms of Quantum efficiency (QE), light and dark IV characteristics. All the simulations were done by the popular one dimensional PV simulator 'Analysis of Micro-electronics and Photonic Structures' (AMPS-1D). The results here indicate that As<sub>2</sub>Te<sub>3</sub> has performed better as a BSF layer with 25.07% of conversion efficiency. Not to mention, the other BSFs also showed good results comparing to the highly efficient CdTe cell reported recently.

(Received December 31, 2018; Accepted April 25, 2019)

*Keywords:* CdTe, Solar cell, AMPS-1D, Simulation, BSF layer

### 1. Introduction

Cadmium Telluride (CdTe) thin film solar cell has already received great attention by researches due to its ideal and direct band gap (1.5 eV), and excellent absorption coefficient ( $>5 \times 10^{15} \text{ cm}^{-1}$ ) and good electrical properties [1-3]. A multi-giga-watt/year production has already been achieved by CdTe thin film photovoltaic manufacturers attributed to achieved high efficiency and lower fabrication cost [4]. Moreover, CdTe thin film solar cells have shown high efficiency and long-term durable performance under AM1.5G illuminations for terrestrial usage [5]. However, to be a sustainable primary energy source, the cost should be reduced further possibly through the increase of conversion efficiency as well as reduction of material usage, cell processing and balance of system costs. Now the highest efficiency of CdTe thin film solar cells is only 21.5%, achieved by First Solar [6] which still far from its theoretical efficiency limit ( $\approx 29\%$ ). Therefore, reducing the thickness ( $\leq 2 \mu\text{m}$ ) of CdTe absorber layer and increase of efficiency towards its theoretical limit by reducing the optical and carrier recombination loss is highly desirable. Carrier recombination could be achieved by formation of a stable and efficient low resistive back contact which still remaining a great challenge for CdTe solar cell.

CdTe has large electron affinity and low carrier concentration. Thus, to make an ohmic contact to CdTe, a metal with a work function greater than 5.7 eV is required, however, no metal have such large work function ( $>5.7\text{eV}$ ) to match properly with CdTe. Thus, there're naturally exist a wide Schottky barrier between the CdTe and Metal back contact. Fahrenbruch and Bube has been extensively reviewed various techniques about the Ohmic contact formation in CdTe solar cells [7]. The popular strategy to make Ohmic contact is to create a heavily p-doped CdTe surface by chemical etching and applying a back surface field (BSF) layer or buffer layer of high

---

\*Corresponding author: aminul.islam@uniten.edu.my

carrier concentration and low resistive between CdTe and the back contact [8]. The barrier width at the back contact interface of CdTe is reduced by this process and a tunnelling barrier formed in this way is quasi ohmic contact. Also, BSF layer works as a minority carrier reflector increase short circuit current and open circuit voltage [8, 9]. Thus, an efficient BSF layer is an inevitable element that helps the cell to achieve higher efficiency. The importance of BSF layers in the field solar cells have been first attracted in the 1980s [10, 11]. The main role of BSF layer is to provide confinement for the photo-generated minority carriers and keep them within the p-n junction area to be efficiently collected. However, BSF layer has to be implement without increasing the series resistance of the device. Additionally, photon confinement capabilities are also an interesting ancillary property for good BSF layer.

The main objective of this study is to find out a higher efficiency and more stable CdTe solar cell by introducing BSF layer. We consider four binary semiconductor as a BSF materials such as  $\text{As}_2\text{Te}_3$ , PbTe, SnTe and GeTe and investigated their impact on performance of CdTe solar cells by Analysis of Microelectronics and Photonic Structures (AMPS 1D). In depth analysis of the effect of having BSFs is also given here including the effect of series and shunt resistances on the cell performance, quantum efficiency (QE), light and dark I-V and hetero-junction band diagram explanations. Also, for understanding the stability and vulnerability of the cell under different environmental conditions via temperature and illumination effect on the cell have also been discussed.

## 2. Methodology

AMPS-1D simulator has been employed in this study. It has been proven to be a very powerful tool in understanding device operation and physics that is designed based on the basic semiconductor equations such as Poisson equation, continuity equation of electrons and holes. AMPS-1D is well adapted to modeling various hetero- and homo-junctions, multi-junction, and Schottky barrier devices [12, 13]. The structure of the employed CdTe solar cell structure in this study is depicted in Fig. 1. Fig. 1(left) and 1(right) shows the structure of conventional CdS/CdTe solar cell and modified with CdS:O/CdTe solar cell with different BSF layers. First, convention n structure has been considered as a base cell, then CdS window layers has been altered by CdS:O and different BSF layers have been inserted. The front contact ZnO:Al and CdS:O layers thickness was fixed to 500 nm and 100 nm, respectively in this study. The absorber layer CdTe has been varied from 100-2000 nm and the change of performance parameters are observed. The all BSF layers thickness have also varied from 100 nm to 1000 nm with fixed CdTe layer thickness of 1000 nm. The operating temperature and light intensity have been changed from 25 °C to 150 °C and 0.01 suns to 1000 suns, respectively. Material parameters set for device simulation are summarized in Table1 were adopted from some standard references [3, 9, 14-16].

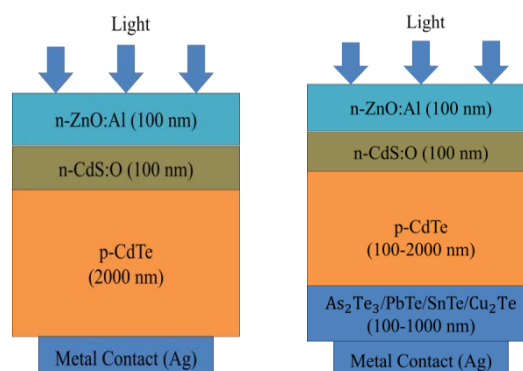


Fig. 1. Schematic structure of the CdTe solar cell (left) conventional and (right) modified structure employed in this study.

Table 1. Parameters used in simulation [3, 9, 14-16].

Parameters	n-ZnO:Al	n-CdS:O	p-CdTe	As <sub>2</sub> Te <sub>3</sub> /PbTe/SnTe/GeTe
Relative permittivity, $\epsilon/\epsilon_0$	9.00	9.00	36.00	20/40/100/36
Electron mobility, $\mu_c$ (cm <sup>2</sup> /Vs)	100	350	100	500/1600/500/100
Hole mobility, $\mu_p$ (cm <sup>2</sup> /Vs)	25	50	20	210/600/2720/120
Donor concentration, $N_D/N_A$ (cm <sup>-3</sup> )	$1.0 \times 10^{18}$	$1.0 \times 10^{16}$	$7.5 \times 10^{15} - 7.5 \times 10^{20}$	$7.5 \times 10^{19}/8 \times 10^{19}/7.5 \times 10^{19}/7.5 \times 10^{20}$
Band gap, $E_g$ (eV)	3.30	1.45	0.8	0.6/0.29/0.18/0.9
Effective density of states in conduction band, $N_C$ (cm <sup>-3</sup> )	$2.2 \times 10^{18}$	$1 \times 10^{19}$	$1.0 \times 10^{16}$	$1 \times 10^{16}$
Effective density of states in valance band, $N_V$ (cm <sup>-3</sup> )	$1.8 \times 10^{19}$	$2.4 \times 10^{18}$	$1.0 \times 10^{17}$	$1 \times 10^{17}$
Electron affinity, $\chi$ (eV)	4.50	4.5	4.80	4/4.6/5.1/4.8
Thickness, W (nm)	500	100	100-5000	100-1000

Table 2. Contact layer parametric values used for simulation.

Parameters	Front contact	Back contact
Barrier height, $\phi_b$ (eV)	1.9	0.03
Electron recombination velocity (cms <sup>-1</sup> )	$1 \times 10^7$	$1 \times 10^7$
Hole recombination velocity (cms <sup>-1</sup> )	$1 \times 10^7$	$1 \times 10^7$
Reflection coefficient	0.2	0.9

### 3. Results and discussion

#### 3.1. Influence of absorber layer thickness

Absorber layer thickness plays an important role in determining the solar cell efficiency. Thickness of the absorber layer affects the diffusion length of carriers. If the absorber layer is very thin, then absorption become less, ultimately efficiency reduces. On the other hand, if the absorber layer is very thick, then the charge carriers may recombine before travel up to the charge collecting layers and efficiency reduces. Thus, optimization of absorber layer thickness is very important to achieve good efficiency. In this investigation the absorber layer thickness for all the cells were changed from 100 nm to 5000 nm. The acceptor concentration of this cell was set constant at  $5 \times 10^{18}$  cm<sup>-3</sup>.

Fig. 2(a) represents short circuit current  $J_{SC}$  for As<sub>2</sub>Te<sub>3</sub>, PbTe, SnTe and GeTe, where  $J_{SC}$  found almost equal and similar for all types of BSF layers (the highest  $J_{SC}$  for PbTe: 27.16 mAcm<sup>-2</sup>, GeTe: 27.47 mAcm<sup>-2</sup>, As<sub>2</sub>Te<sub>3</sub>: 27.09 mAcm<sup>-2</sup> and SnTe: 26.93 mAcm<sup>-2</sup>). It is evident from the figure that  $J_{SC}$  rises to an optimal value of  $\approx 27$  mAcm<sup>-2</sup> at 900-1000 nm thickness and then saturates with very slight decay as thickness increases. In terms of  $V_{OC}$  and efficiency, As<sub>2</sub>Te<sub>3</sub> shows the highest result with 1.18V and 25.06%, respectively. For the rest three BSFs where, PbTe shows 1.09V, SnTe shows 1.11V and GeTe shows 1.09V. The relative decrease in  $V_{OC}$  is not very significant after 1000 nm of CdTe layer thickness. Decreasing the reverse saturation current is responsible for fill factor increasing by reducing the recombination of the charge carriers. Fig. 2(c), illustrates SnTe has better fill factor (88%) but less open circuit voltage that's why generates low efficiency considering others. Table 3 shows the highest performance of solar cells with different BSF layers.

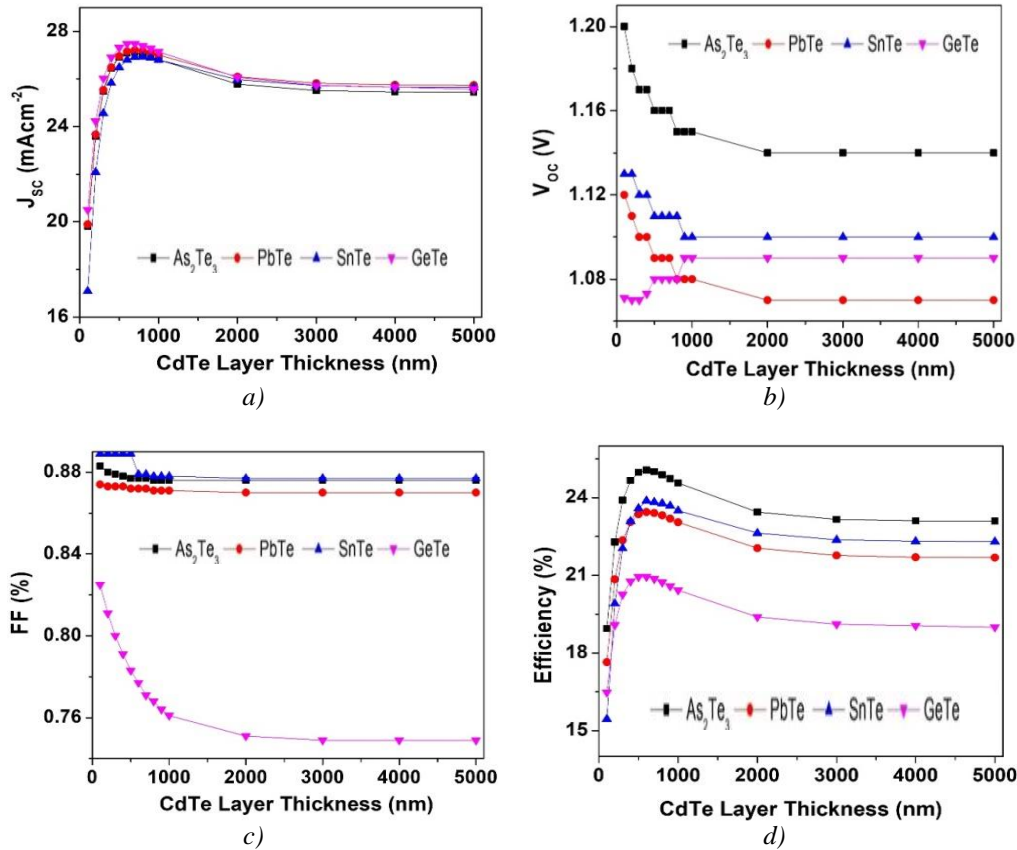


Fig. 2. Influence of CdTe absorber layer thickness on (a)  $J_{sc}$ , (b)  $V_{oc}$ , (c) FF and (d) Efficiency (BSF layers thickness was fixed at 100nm).

Table 3. Associated highest performance for solar cell with different BSF layers.

Structures	$J_{sc}$ ( $\text{mAcm}^{-2}$ )	$V_{oc}$ (V)	FF	Efficiency (%)
ZnO:Al/CdS:O/CdTe/As <sub>2</sub> Te <sub>3</sub>	27.09	1.16	0.88	25.06
ZnO:Al/CdS:O/CdTe/PbTe	27.16	1.09	0.87	23.45
ZnO:Al/CdS:O/CdTe/SnTe	26.80	1.11	0.88	23.89
ZnO:Al/CdS:O/CdTe/GeTe	27.48	1.08	0.78	20.95

### 3.2. Influence of BSF Layer Thickness

The purpose of inserting BSF layer is to decrease probable recombination loss and the barrier height at the back contact of proposed cell. Fig. 3 shows the performance of CdTe solar cell with the changing thickness of BSF layer where CdTe layer thickness was fixed at 1000 nm. Arsenic Telluride (As<sub>2</sub>Te<sub>3</sub>) having higher band gap comparing PbTe and SnTe which helps to arrogance back the electrons from the CdTe/As<sub>2</sub>Te<sub>3</sub> junction and thus would pay in the improvement of carrier recombination. Though GeTe has the highest band gap of 0.9eV, it is however unable to show better efficiency. In Fig. 3(a) Cell with PbTe (27.16  $\text{mAcm}^{-2}$ ) is lesser than GeTe (27.47  $\text{mAcm}^{-2}$ ) but greater than As<sub>2</sub>Te<sub>3</sub> (27.09  $\text{mAcm}^{-2}$ ) and SnTe (26.934  $\text{mAcm}^{-2}$ ). But when it comes to the efficiency in Fig. 3(b), As<sub>2</sub>Te<sub>3</sub> seems to have the highest efficiency of 25.06% while PbTe shows 23.45%, SnTe shows 23.89% and GeTe shows efficiency of 20.95%. Which undoubtedly says that As<sub>2</sub>Te<sub>3</sub> is best matched BSF with 100 nm of thickness.

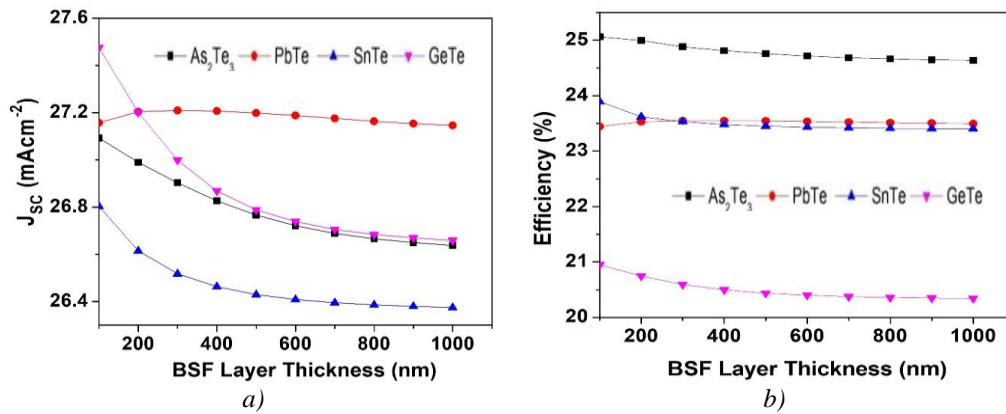


Fig. 3. Effect of BSF layer thickness on (a)  $J_{sc}$  and (b) efficiency.

The quantum efficiency (QE) can be defined as the ratio of the current of photo-generated carriers to the incident photon flux. The QE of a solar cell strongly depends on the energy of the individual photon. This may be due to both the wavelength dependency of the optical absorption coefficients in semiconductors and the depth dependency of the carrier collection probability. The fig. 4 here depicts the quantum efficiency of CdTe Solar cell with different BSF layers. The wavelength here was considered from 400nm to 900nm. From the figure it is clear that all the cells provide almost same result. But a closer look can determine that the cell with GeTe layer shows slightly better performance. In the low wavelength region all the cells gives almost exact same performance. But under the mid-range wavelength GeTe shows better result than  $As_2Te_3$ , PbTe and SnTe. This is, may be, because of diffusion length in CdTe cell with GeTe layer which is slightly higher than the others. However, every cell shows more than 93% efficiency for the whole visible spectra.

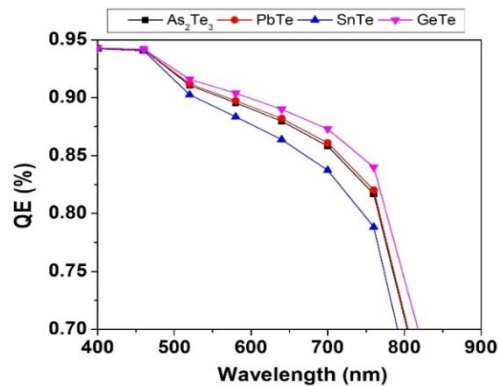


Fig. 4. Quantum efficiency of CdTe solar cell with different BSF layers.

Fig. 5 shows the dark I-V curve for each cell used in this study. The diode characteristic parameters such as ideality factor, series ( $R_s$ ) and shunt resistance ( $R_{sh}$ ) can be determined from the curves obtained from simulation.  $R_s$  and  $R_{sh}$  were extracted from the dark I-V curves where  $R_s$  was obtained from the high voltage region and  $R_{sh}$  was obtained from the low voltage region. Table 3 shows the values of resistances obtained from the figure.

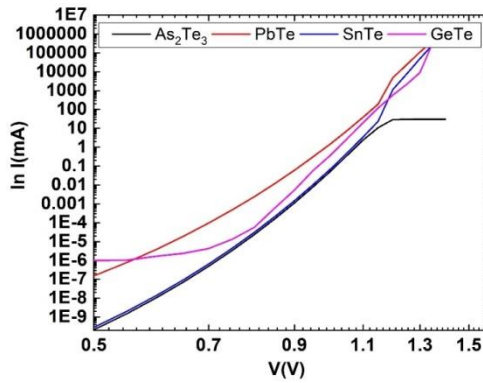


Fig. 5. Dark I-V characteristics curve for different cell structures.

Table 3. Series and Shunt resistances for different cell structures.

Cell with BSF	As <sub>2</sub> Te <sub>3</sub>	PbTe	SnTe	GeTe
Series Resistance, R <sub>S</sub> (Ω)	4.78	2.12	3.00	3.60
Shunt Resistance, R <sub>Sh</sub> (kΩ)	7.49	0.56	2.17	1.11

From the Fig. 5 and Table 3 it is clear that all cells maintain low R<sub>S</sub> at higher voltage region and higher R<sub>Sh</sub> at low voltage region. In terms of resistivity, the cell with As<sub>2</sub>Te<sub>3</sub> BSF shows the lowest R<sub>S</sub> and highest R<sub>Sh</sub> which implies that the performance of this cell is better than the other three. On the other hand, the cell with PbTe cell shows the lowest R<sub>Sh</sub> among the three structures. The behavior of the cells can also be understood from the band diagram of the cells in Fig. 6. The cell with GeTe BSF layer shows moderate behavior with R<sub>S</sub> of 3.6Ω and R<sub>Sh</sub> of 1.11 kΩ. All four cells exhibit very good performance in terms of minority carrier reflection. Among all the cells, As<sub>2</sub>Te<sub>3</sub> shows higher R<sub>Sh</sub> than others as the valence band offset is bigger than the rest two which ensures the highest shunt resistance. Also, the cell with As<sub>2</sub>Te<sub>3</sub> BSF has the larger conduction band offset which acts as a good minority carrier reflector.

Fig. 7 shows the simulated light J-V curve for each cell. Each of the cells has the BSF layer of 100 nm. Each curve describes the cell characteristics with J<sub>SC</sub>, V<sub>OC</sub> and FF. From the figure it is clear that the cell with GeTe cell has the highest J<sub>SC</sub>, whereas, the most efficient cell is the cell with As<sub>2</sub>Te<sub>3</sub> BSF. However, all the cell secured high FF which may be is due to improved back contact orientation and carrier recombination on the back surface.

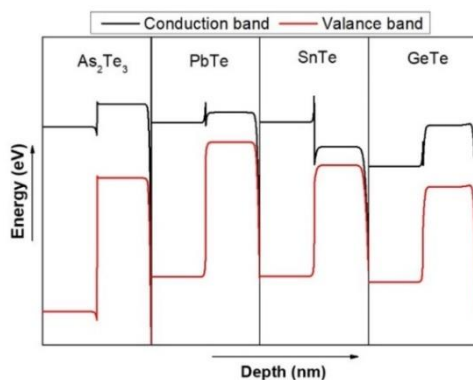


Fig. 6. Band diagram of CdTe solar cell with different BSF layers.

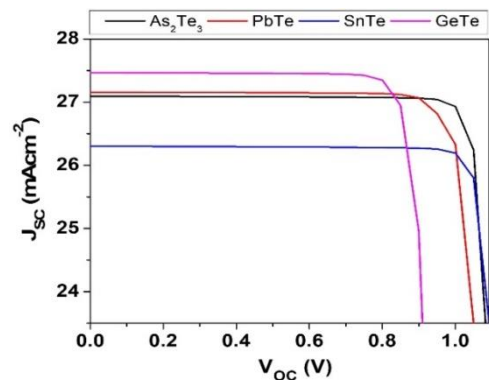


Fig. 7. Light J-V characteristics curve of CdTe solar cells with different BSF layers.

### 3.3. Influence of temperature

The permanence of the cells at different temperature has been investigated because it believe that temperature plays a vital role on cell's performance and stability. At higher operating temperature, parameters such as the electron and hole mobility, carrier concentrations, density of states and band gaps of the materials are affected [17]. The performance, and cell thermal stability has been investigated to know the effects of higher operating temperature with BSF layer. Simulation was performed for operating temperature ranged from 298K to 450K as shown in fig. 8 (a) and (b). As the cell operating temperature increased, the band gap decreases, and hence the cell responds to longer wavelength portions of the spectrum, and therefore the short circuit current actually increases but little with operating temperature [18]. In addition, the decreases of Voc with temperature as shown in Fig. 8 (a) indicating the temperature dependence reverse saturation current of the solar cell. The equation for reverse saturation current is:

$$I_0 = qA \frac{Dn_i^2}{LN_d} \quad (1)$$

The parameters have their usual meanings. In eqn. (1), it is seen that the saturation current is significantly affected by the intrinsic carrier concentration ( $n_i$ ). As an impact of high temperature bandgap is reduced and consecutively, lower band gaps giving a higher intrinsic carrier concentration, i.e., higher temperatures results the higher  $n_i$  and reduced Voc as seen in Fig. 8 (a). As the  $V_{OC}$  changes contributing most of the variation in efficiency and hence, decreasing the efficiency of the cell with the increase of temperature is clearly observed in Fig 8 (b).

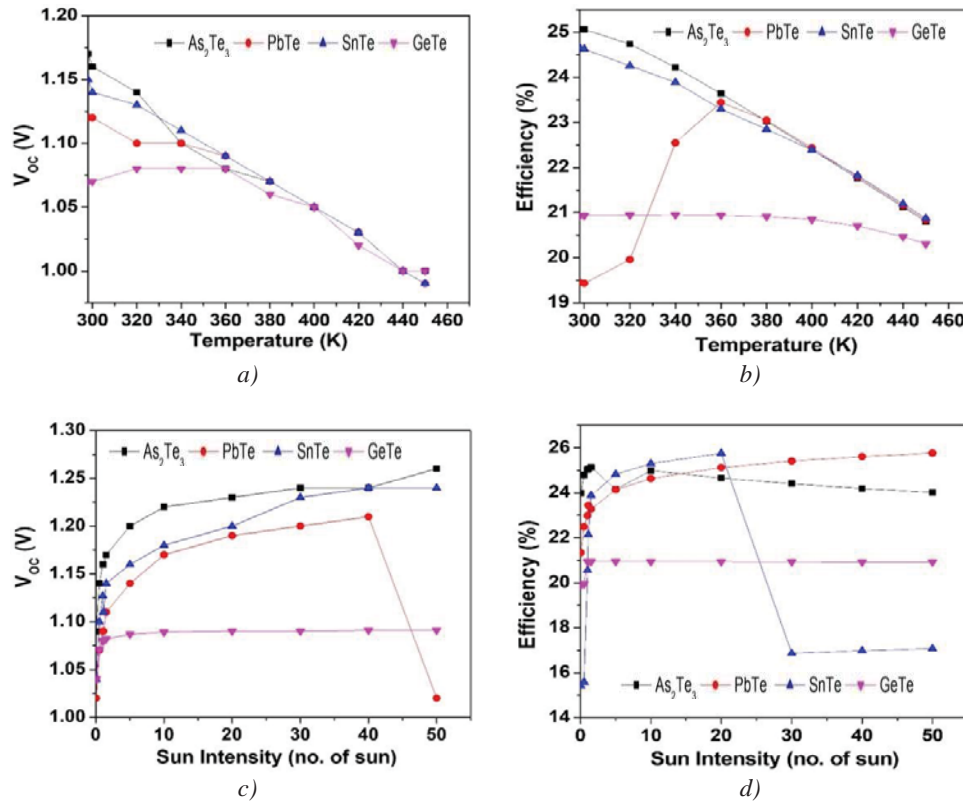


Fig. 8. Effect of temperature on (a)  $V_{OC}$  and (b) efficiency, and effect of sun intensity on (c)  $V_{OC}$  and (d) efficiency.

The temperature coefficients of the solar cells with BSF of As<sub>2</sub>Te<sub>3</sub>, PbTe, SnTe and GeTe are found to be 0.07%, 0.07%, 0.09% and 0.02% respectively. It could be seen that As<sub>2</sub>Te<sub>3</sub> has

represented better open circuit voltage (1.17V) and efficiency (25.07% at 298K) against temperature than others by the moderate temperature coefficient of 0.07%. On the other hand, GeTe shows a stable efficiency of around 20.49% with the increase of temperature until 420K. The overall results once again states that As<sub>2</sub>Te<sub>3</sub> to be the most deserving BSF for CdTe solar cell.

### 3.4. Influence of Sun Intensity

The illumination covers a huge part on the performance analysis of solar cells as the module has to be under direct sun light. As during day time also, the sun does not remain the same, thus, the effect of sun intensity has to be analyzed to ensure better performance. Sun intensity can be very vital towards the solar cell output as it can change the parameters such as the J<sub>SC</sub>, V<sub>OC</sub>, FF and also efficiency itself. The main factor of solar cell that is affected by sun intensity is the series and shunt resistance. In this analysis, the sun intensity of sun was changed from 0.01sun to 100suns. From fig. 8 (c) it is seen that the cell with As<sub>2</sub>Te<sub>3</sub> provides better open circuit voltage than the cells with PbTe, SnTe and GeTe. With the increase of sun intensity, the V<sub>OC</sub> kept on increasing for all the cell structures. It is known to that the Voc is increases logarithmically with the increase of light intensity, as shown in the equation below:

$$V'_{oc} = V_{oc} + \frac{nkT}{q} \ln x \quad (2)$$

where x is the number of sun and other parameters have their usual meaning. On the other hand, in fig. 8(d), it is seen that the efficiency of the solar cells with BSF of As<sub>2</sub>Te<sub>3</sub>, PbTe, and GeTe showed almost stable in low light condition indicating their high shunt resistance for which a greater fraction of its original power is retained under low illumination [19]. On the other hand, the cell with SnTe BSF, in which efficiency drastically increase after 0.5 sun and start to decrease above the sun intensity of 20 sun. May be it is because of series resistance which reduced highly after 0.5 sun and increase again after 20 sun. Finally, at standard condition, i.e. 1 sun (at AM1.5 or 1 KW/m<sup>2</sup>) the efficiency achieved by the cells are 25.04% for CdTe/As<sub>2</sub>Te<sub>3</sub>, 22.98% for CdTe/PbTe, 23.89% for the structure CdTe/SnTe and 20.95% for CdTe/GeTe.

## 4. Conclusions

In this study, four different structures of CdTe solar cell were taken under consideration, where, every structure provides good performance working as a BSF layer. The simulation process with AMPS 1D describes the performance of cells in terms of thickness, temperature and sun intensity. Also characterization of I-V characteristics and quantum efficiency were also analyzed. SnTe as a BSF layer showed high shunt resistance and moderate series resistance. It acts very wisely with the CdTe absorber layer as a good minority carrier reflector. Its high conduction band offset is very much capable of mitigating the series resistance problems and showing better performance. Contrariwise, PbTe showed less shunt resistance, which proves to be the moderate performer with the CdTe absorber layer but GeTe shows the lowest performance here with the less conversion efficiency. As<sub>2</sub>Te<sub>3</sub> however shows the best performance with CdTe with highest R<sub>Sh</sub> and good result in quantum efficiency. The reason why its R<sub>S</sub> is higher than others is because of the higher valance band offset with absorber layer (CdTe). The minority carrier reflection works very fine and gives 25.061% efficiency. Considering the quantum efficiency, I-V characteristics and performance under changing temperature and sun it is clear that As<sub>2</sub>Te<sub>3</sub> is the best performed BSF layer for CdTe solar cell.

## Acknowledgment

This work has been supported by the Department of Electrical and Electronic Engineering, International Islamic University Chittagong, Chittagong 4314, Bangladesh.

## References

- [1] M. A. Green, K. Emery, Y. Hishikawa, W. Warta, E. D. Dunlop, *Progress in Photovoltaics: Research and Applications* **23**, 1 (2015).
- [2] A. Morales-Acevedo, Can we improve the record efficiency of CdS/CdTe solar cells?
- [3] N. Amin, K. Sopian, M. Konagai, *Solar Energy Materials and Solar Cells* **91**, 1202 (2007).
- [4] M. A. Islam, K. S. Rahman, K. Sobayel, T. Enam, A. M. Ali, M. Akhtaruzzaman, N. Amin, *Solar Energy Material and Solar Cells* **172**, 384 (2017).
- [5] Tetsuya Aramoto, Seiji Kumazawa, Hiroshi Higuchi, Takashi Arita, Satoshi Shibutani, Tuyoshi Nishio, Junji Nakajima, Miwa Tsuji, Akira Hanafusa, Takeshi Hibino, *Japanese Journal of Applied Physics*, **36**(10R), 6304.
- [6] M. A. Green, K. Emery, Y. Hishikawa, W. Warta, E. D. Dunlop, *Prog. Photovolt: Res. Appl.* **24**, 905 (2016).
- [7] A. Fahrenbruch, R. Bube, Elsevier, 2012.
- [8] J. Sarlund, M. Ritala, M. Leskela, E. Siponmaa, R. Zilliacus, *Solar Energy Materials and Solar Cells* **44**, 177 (1996).
- [9] M. A. Islam, Y. Sulaiman, N. Amin, *Chalcogenide Letters* **8**(2), 65 (2011).
- [10] D. L. Batzner, A. Romeo, H. Zogg, R. Wendt, A. N. Tiwari, *Thin Solid Films* **387**, 151 (2001).
- [11] D. Kraft, A. Thissen, J. Broetz, S. Flege, *Journal of Applied Physics* **94**, 3589 (2003).
- [12] M. A. A. Noman, M. S. Islam, M. J. Abden, M. Arifuzzaman, M. A. Islam, In *Innovations in Science, Engineering and Technology (ICISSET)*, 2016, Chittagong, pp. 1-4.
- [13] Hong Zhu, Ali Kaan Kalkan, Jingya Hou, Stephen J. Fonash, *AIP Conference Proceedings* **462**, 309 (1999).
- [14] M. A. Matin, Mrinmoy Dey, 3rd International Conference on Informatics, Electronics & Vision, Dhaka, 2014, pp. 1-5.
- [15] M. Dey, M. A. Matin, N. Amin, 18th International Conference on Computer and Information Technology (ICCIT), Dhaka, 2015, pp. 573-576.
- [16] M. Dey, M. A. Matin, *International Journal of Research in Computer Engineering & Electronics* **4**(2), 2015.
- [17] J. C. Fan, *Solar Cells* **17**(2-3), 309 (1986).
- [18] V. L. Dalal, A. R. Moore, *Journal of Applied Physics* **48**(3), 1244 (1997).
- [19] G. Bunea, K. Wilson, Y. Meydbray, M. Campbell, D. D. Ceuster, 4th World Conference on Photovoltaic Energy Conference, Waikoloa, HI, 2006, pp. 1312–1314.